NATIONAL ADVISORY COMMITTEE FOR AERONAUTICS

TECHNICAL NOTE 3480

FREE-SPINNING-TUNNEL INVESTIGATION OF GYROSCOPIC EFFECTS

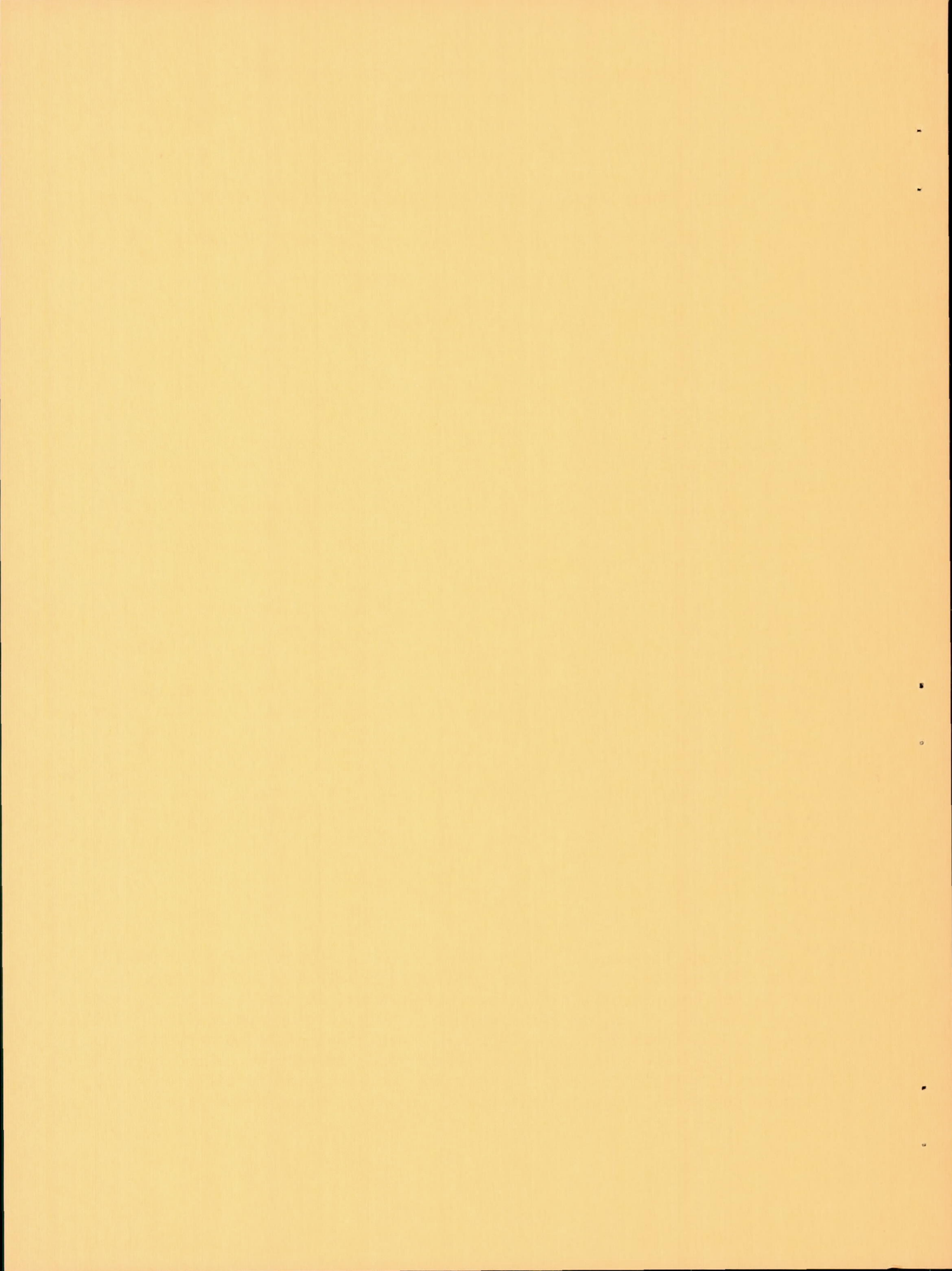OF JET-ENGINE ROTATING PARTS (OR OF ROTATING PROPELLERS)

ON SPIN AND SPIN RECOVERY

By James S. Bowman, Jr.

Langley Aeronautical Laboratory
Langley Field, Va.

NACA

Washington

August 1955

NATIONAL ADVISORY COMMITTEE FOR AERONAUTICS

TECHNICAL NOTE 3480

FREE-SPINNING-TUNNEL INVESTIGATION OF GYROSCOPIC EFFECTS

OF JET-ENGINE ROTATING PARTS (OR OF ROTATING PROPELLERS)

ON SPIN AND SPIN RECOVERY

By James S. Bowman, Jr.

SUMMARY

An investigation has been initiated in the Langley 20-foot free-spinning tunnel to study the gyroscopic effects of jet-engine rotating parts (or of rotating propellers) on the erect spin and spin-recovery characteristics. A 1/21-scale model of a military attack airplane was arbitrarily used, and tests were made at a basic loading (mass distributed chiefly along the fuselage) and at alternate loadings (additional mass distributed along the wings).

The angular momentum of the rotating parts was simulated on the model by a rotating flywheel powered by a model airplane engine. The rotating flywheel (clockwise as viewed from cockpit) generally caused the model to spin at a decreased angle of attack and an increased rate of rotation in right spins, and at an increased angle of attack and a decreased rate of rotation in left spins. For the basic loading, rotating the flywheel generally changed the recovery characteristics from satisfactory to unsatisfactory for right spins, but for left spins the satisfactory recovery characteristics obtainable with the flywheel not rotating were not appreciably altered. For the alternate loadings, rotating the flywheel had, in general, little discernible net effect on recovery characteristics.

INTRODUCTION

Although the general policy for either intentional or accidental spins has been to cut off power as soon as possible after the spin is initiated, because of possible adverse effects, in some instances pilots have flown out of an otherwise uncontrollable spin by application of full power in a propeller-driven airplane. Such results from power-on spins may possibly have been due to increased effectiveness of controls in the slipstream. For a jet engine, however, the situation is different, and unpublished data indicate that the thrust alone might be of little

assistance. For both propeller-driven and jet-propelled airplanes, spin
and spin-recovery characteristics may differ for power-on and power-off
conditions, as well as for power-on spins to the right and to the left.
These differences may at times have caused serious difficulty in recov-
ering from spins in one direction, whereas recoveries from spins in the
other direction could be readily achieved. The differences in spins and
recoveries may have been due in part to the gyroscopic moments produced
by rotating propellers or rotating parts of jet engines. For a jet-
propelled airplane, the rotating parts of the engine may continue to
rotate at nearly full speed for a long time after power is cut off because
of angular momentum.

The present preliminary investigation has been made to determine
the gyroscopic effects of jet-engine rotating parts (or of rotating pro-
pellers) on the erect spin and recovery characteristics of a model of
a military attack airplane. Tests were conducted in the Langley 20-foot
free-spinning tunnel, and the gyroscopic moments were obtained on the
model by means of a rotating flywheel powered by a model airplane engine.
Tests with power on and power off were made for both right and left spins
at a basic mass loading (mass distributed chiefly along the fuselage)
and at alternate loadings (additional mass distributed along the wings).
The tests covered a range of control configurations. An analysis of the
model results is presented in an attempt to explain the effects of the
flywheel rotation on the behavior of the model during spins and recoveries.

SYMBOLS

The body system of axes is used in this paper. A sketch indicating
positive directions of moments and angular velocities is shown in fig-
ure 1.

b wing span, ft

S wing area, sq ft

$\bar{c}$ mean aerodynamic chord, ft

$x/\bar{c}$ ratio of distance of center of gravity rearward of leading
                edge of mean aerodynamic chord to mean aerodynamic chord

$z/\bar{c}$ ratio of distance between center of gravity and reference
                line to mean aerodynamic chord, positive when center of
                gravity is below reference line

m mass of airplane, slugs

I_X, I_Y, I_Z moments of inertia about X-, Y-, and Z-axes, respectively, slug-ft^2

I_p polar moment of inertia of flywheel, slug-ft^2

$\dfrac{I_X - I_Y}{mb^2}$ inertia yawing-moment parameter

$\dfrac{I_Y - I_Z}{mb^2}$ inertia rolling-moment parameter

$\dfrac{I_Z - I_X}{mb^2}$ inertia pitching-moment parameter

ρ air density, slugs/cu ft

μ airplane relative-density coefficient, $m/\rho Sb$

α angle between reference line and vertical (approximately equal to absolute value of angle of attack at plane of symmetry), deg

ϕ angle between Y-axis and horizontal, deg

V full-scale rate of descent, ft/sec

Ω full-scale angular velocity about spin axis, radians/sec except on charts where revolutions per second (rps) is used

p angular velocity in roll, radians/sec

q angular velocity in pitch, radians/sec

r angular velocity in yaw, radians/sec

L rolling moment, ft-lb

M pitching moment, ft-lb

N yawing moment, ft-lb

p' angular velocity of flywheel, radians/sec

Subscripts:

i inertia

aero   aerodynamic

APPARATUS AND METHODS

Model

As previously indicated, a 1/21-scale dynamic model of a military attack airplane was arbitrarily used in the investigation. The angular momentum of the full-scale rotating engine parts or propellers was simulated by a rotating flywheel powered by a model airplane engine located so that the axis of the angular momentum was parallel to that of the corresponding airplane. The flywheel rotated clockwise when viewed from the pilot's position. No attempt was made to simulate the slipstream effect of a propeller. A three-view drawing of the model as tested, showing the engine and flywheel mounted on the model, is presented in figure 2. The dimensional characteristics of the airplane which corresponds to the 1/21-scale model investigated are presented in table I. The model was ballasted to obtain dynamic similarity to the corresponding airplane at an altitude of 15,000 feet (ρ = 0.001496 slug/cu ft). Mass characteristics and inertia parameters for the basic loading and the alternate loadings 1 and 2 are presented in table II; also presented is the inertia of the engine represented. A remote-control mechanism was installed in the model to actuate the controls for the recovery attempts.

Wind Tunnel and Testing Technique

The tests were conducted in the Langley 20-foot free-spinning tunnel; operation of the tunnel is generally similar to that of the free-spinning tunnel described in reference 1, except that the model launching technique for the spin tests has been changed. With the controls set in the desired position, the model is launched by hand with rotation into the vertically rising airstream. After a number of turns in the established spin, the recovery is attempted by moving one or more model controls by means of the remote-control mechanism. After recovery, the model dives into a safety net. A photograph of the model during a spin is shown in figure 3.

Based on spin-tunnel experience, recovery characteristics of a model are generally considered satisfactory if, after movement of controls, rotation stops within two turns for the spin with the normal spin-control configuration (ailerons neutral, elevator full up, and rudder full with spin), and if slight deviation of controls (ailerons deflected one-third in the adverse direction, elevator two-thirds of full up, and rudder moved to only two-thirds of full against spin) does not increase the turns required for recovery beyond $2\frac{1}{4}$. For the present investigation, recovery characteristics were considered satisfactory if recoveries from all spins with elevators up (ailerons with the spin, neutral, and against

the spin), as well as from the spin with elevator and ailerons neutral,
took place within $2\frac{1}{4}$ turns. For recovery attempts in which a model
strikes the safety net while still in a spin, the recovery is recorded
as greater than the number of turns made from the time the controls
were moved to the time the model struck the net (for example, >3). A
>3-turn recovery does not necessarily indicate an improvement over a
>7-turn recovery. For recovery attempts in which the model does not
recover within 10 turns before striking the net, the recovery results
are generally recorded as ∞.

For the tests in which the model was launched with the flywheel
rotating, the flywheel was brought up to full speed before the model
was launched into the tunnel.

PRECISION

The test results presented herein are believed to be the true
values given by the model within the following limits:

α, deg . . . . ±1
∅, deg . . . . ±1
V, percent . . . . ±5
Ω, percent . . . . ±2

Turns for recovery:
  When obtained from motion-picture records . . . . ±1/4
  When obtained by visual estimate . . . . ±1/2

These limits may have been exceeded for certain spins in which it was
difficult to control the model in the tunnel because of the wandering
or oscillatory nature of the spin.

Because of inadvertent changes in the model due to minor repairs,
such as are customarily made during tests of free-spinning models, the
measured weight and mass distribution of the model varied from the orig-
inal values listed in table II within the following limits:

Weight, percent . . . . 0 to 1 low
Center-of-gravity location, percent c̄ . . . . 0 to 2 rearward

Moments of inertia, percent:
  I_X . . . . 1 to 3 low
  I_Y . . . . 0 to 4 high
  I_Z . . . . 0 to 2 high

The accuracy of measuring weight and mass distribution is believed to be within the following limits:

Weight, percent . . . . ±1
Center-of-gravity location, percent c̄ . . . . ±1
Moments of inertia, percent . . . . ±5

TEST CONDITIONS

All tests were conducted with the flaps and landing gear retracted and the cockpit closed. The design included fixed extended slats. For each control configuration used, tests were made alternately with the flywheel not rotating and with the flywheel rotating. The rotation of the flywheel was such as to simulate the engine parts of a full-scale airplane which are rotating at 3,000 revolutions per minute, within approximately ±5 percent.

The control configurations used during spins for all loadings were up-elevator settings with ailerons neutral, ailerons against the spin (stick left in a right spin), and ailerons with the spin; and elevator-neutral and elevator-down settings with ailerons neutral. For the alternate loadings, some tests were also made with ailerons against the spin and with the spin when the elevators were neutral and down. Recoveries were attempted by rapid reversal of the rudder from full with to full against the spin. The tail fin was set at an angle of 3° with the center line of the model, the leading edge was to the left, and the rudder deflections were measured from the fin plane.

Control deflections used on the model during the tests (measured perpendicular to the hinge lines) were as follows:

Rudder, deg . . . . 28 right, 28 left
Elevator, deg . . . . 25 up, 15 down
Ailerons, deg . . . . 17 up, 13 down

RESULTS AND DISCUSSION

The results of the model tests are presented in charts 1 to 6. Rate of descent, angle of attack, rate of rotation, angle of wing tilt during the developed spin, and number of turns for recovery are presented for right and left spins with the flywheel rotating and not rotating for each configuration tested. In the charts, the center blocks represent spins with neutral controls. Arrows extending vertically from the center blocks indicate elevator settings for top and bottom rows of blocks; horizontal arrows indicate aileron settings for columns on right and left.

The effect of flywheel rotation (rotation clockwise when viewed from the pilot's position) for right spins generally was to decrease the angle of attack and to increase the rate of rotation for all loading conditions tested. For left spins, flywheel rotation increased the angle of attack and decreased the rate of rotation.

For the basic loading with the mass distributed chiefly along the fuselage, rotation of the flywheel for right spins changed the recovery characteristics from satisfactory to unsatisfactory (chart 1). For left spins (chart 2) the satisfactory recovery characteristics were, in general, affected very little. For the alternate loadings with additional mass distributed along the wings, recovery characteristics which were, in general, already unsatisfactory remained unsatisfactory when the flywheel was rotating.

In general, for all loadings with the flywheel not rotating, left spins were steeper than the corresponding right spins and recoveries from the left spins were faster. This may be attributable at least in part to the fin angle and corresponding asymmetric rudder deflection to the right and left, relative to the plane of symmetry of the model.

As an aid in explaining the effects of flywheel rotation on the behavior of the model during spins and recoveries, an analysis was made of the moments produced during the spin by the spinning mass of the airplane (gyrodynamic inertia moments) and the moments produced by the rotation of the flywheel about its own axis (gyroscopic inertia moments). The relationships between the gyrodynamic and gyroscopic inertia moments are indicated by the equations

$$N_i \equiv \left(I_X - I_Y\right)pq + I_p p'q \tag{1}$$

$$L_i \equiv \left(I_Y - I_Z\right)qr \tag{2}$$

$$M_i \equiv \left(I_Z - I_X\right)rp - I_p p'r \tag{3}$$

Equations (1), (2), and (3) are based on the assumption of a fully developed steady spin which is without oscillations and is about a vertical spin axis. The steepening of the right spins and the flattening of the left spins caused by the flywheel rotation may be explained in part by using equation (3). This equation (written for a right spin) represents the sum of the gyrodynamic inertia moments from reference 2 (first term on right-hand side) and the gyroscopic inertia moments (second term on right-hand side). The gyroscopic moment acts in a nose-down direction, whereas the gyrodynamic moment acts in a nose-up direction. For the left spin, the gyroscopic moment and the gyrodynamic moment both act in a nose-up direction.

The changes which occurred in the rate of spin rotation Ω as a result of the flywheel rotation may be explained by

$$-M_{aero} = \left(I_Z - I_X\right)rp - I_p p'r \tag{4}$$

which is the pitching-moment equation of motion for a developed spin with the flywheel rotating. Since the aerodynamic pitching moment is equal and opposite in sign to the complete inertia pitching moment (eq. (3)), equation (4) is obtained by setting the aerodynamic pitching moment equal to equation (3).

By substituting approximate values for p and r

$$p \approx \Omega \cos \alpha$$

and

$$r \approx \Omega \sin \alpha$$

equation (4) may be expressed for a right spin as

$$-M_{aero} = \left(I_Z - I_X\right)\Omega^2 \frac{\sin 2\alpha}{2} - I_p p'r \tag{5}$$

The aerodynamic pitching moment generally acts in a nose-down (negative) direction in a spin and, therefore, $-M_{aero}$ becomes $-\left(-M_{aero}\right)$, or M_{aero}.

Solving equation (5) for Ω gives

$$\Omega = \left[\frac{M_{aero} + I_p p'r}{\left(I_Z - I_X\right)\frac{\sin 2\alpha}{2}}\right]^{1/2} \tag{6}$$

Thus, for a right spin the aerodynamic pitching moment and the gyroscopic inertia moment in equation (6) are additive and should increase Ω, the rate of rotation. For a left spin, r is negative and the numerator of equation (6) would be $M_{aero} - I_p p'r$; thus, the terms are subtractive and the rate of rotation should decrease.

Spin-tunnel experience has indicated that the yawing moment acting in the spin may be a primary factor in determining what the recovery characteristics will be. As suggested in reference 3, a parameter showing

the manner in which the mass is distributed in the airplane, that is, whether it is distributed primarily along the fuselage or along the wings, may oftentimes be used as an indication of the anticipated effect. On this basis alone, recoveries in which the rudder is reversed may be expected to be affected by the resulting increment in pitching velocity Δq due to the rotating flywheel. For right spins with the basic loading, the corresponding increment in the gyrodynamic yawing moment ΔN (where $\Delta N = \left(I_X - I_Y\right) p \, \Delta q$) would be positive (pro-spin) and therefore would have an adverse effect on recoveries because of a negative (nose-down) increment in q. For left spins, the increment in ΔN would be anti-spin. For the basic loading with flywheel rotating, the differences in recovery characteristics for right and left spins could be considered consistent with this reasoning, but on the basis of the results on all the charts, many other factors such as angle of attack, rate of rotation, and other cross-couple terms, for example, $\left(I_Z - I_X\right) rp$, can influence the results and may make prediction of the net effect of engine rotating parts difficult. It appears that, in order to get the net effect on a specific design, dynamic tests in the spin tunnel will be necessary, at least until more research results become available.

SUMMARY OF RESULTS

A preliminary investigation in the Langley 20-foot free-spinning tunnel to determine the effects of gyroscopic moments produced by a rotating flywheel (clockwise as viewed from cockpit) on the erect spin and spin-recovery characteristics of a 1/21-scale model of a military attack airplane has yielded the following results:

1. For all loading conditions tested, the rotating flywheel generally caused the model to spin at a decreased angle of attack and an increased rate of rotation in right spins, and at an increased angle of attack and a decreased rate of rotation in left spins.

2. For the basic loading with the mass distributed chiefly along the fuselage, recovery characteristics were, in general, changed from satisfactory to unsatisfactory for right spins when the flywheel was rotated. For left spins, the satisfactory recovery characteristics obtainable with the flywheel not rotating were not discernibly altered when the flywheel was rotating.

3. For the alternate loadings with additional mass distributed along the wings, rotating the flywheel had, in general, little discernible net effect on recovery characteristics.

4. It appears that, in order to determine the net effect of rotating engine parts (or rotating propellers) on the recovery characteristics for a specific airplane, dynamic spin-tunnel tests of a model will be necessary.

Langley Aeronautical Laboratory,
    National Advisory Committee for Aeronautics,
        Langley Field, Va., June 21, 1955.

REFERENCES

1. Zimmerman, C. H.: Preliminary Tests in the N.A.C.A. Free-Spinning
    Wind Tunnel. NACA Rep. 557, 1936.

2. Jones, B. Melvill: Dynamics of the Airplane. The Spin. Vol. V of
    Aerodynamic Theory, div. N, ch. VIII, sec. 4, W. F. Durand, ed.,
    Julius Springer (Berlin), 1935, p. 207.

3. Neihouse, A. I.: A Mass-Distribution Criterion for Predicting the
    Effect of Control Manipulation on the Recovery From a Spin. NACA
    WR L-168, 1942. (Formerly NACA ARR, Aug. 1942.)

TABLE I.- DIMENSIONAL CHARACTERISTICS OF THE

AIRPLANE CORRESPONDING TO THE 1/21-SCALE

MODEL INVESTIGATED

Overall length, ft 37.96

Tail-damping power factor . . . . 906 × 10^{-6}

Wing:
  Span, ft 50.19
  Area, sq ft 400.3
  Airfoil section:
    Root chord . . . . NACA 2417
    Tip chord . . . . NACA 4413
  Mean aerodynamic chord, $\bar{c}$, in. 100.05
  Distance from leading edge of wing rearward to leading
    edge of mean aerodynamic chord, in. 14.125
  Incidence:
    Root, deg 3.75
    Tip, deg 0.25
  Dihedral, deg 6

Ailerons:
  Area (rear of hinge line), sq ft 33.4
  Distance from hinge line to trailing edge (outboard tip),
    percent chord 19.0
  Span, percent wing span 48.6

Horizontal-tail surfaces:
  Total area, sq ft 86.97
  Span, ft 19.83
  Elevator area (rear of hinge line), sq ft 22.3
  Distance from normal center of gravity to elevator hinge
    line, ft 22.47
  Airfoil section . . . . NACA 0012-64 (modified)

Vertical-tail surfaces:
  Fin angle (leading edge to left), deg 3
  Total area, sq ft 39.9
  Total rudder area (rear of hinge line), sq ft 19.66
  Distance from normal center of gravity to rudder
    hinge line, ft 23.73
  Airfoil section . . . . NACA 0013 (modified)

TABLE II.- MASS CHARACTERISTICS AND INERTIA PARAMETERS

FOR LOADINGS TESTED ON MODEL

[Values given are full-scale, and moments of inertia
are given about center of gravity.]

Loading	Weight, lb	Center-of-gravity location		Relative-density coefficient, μ, at -	
		$x/\bar{c}$	$z/\bar{c}$	Sea level	Altitude
Basic loading	16,949	0.2844	0.115	11.02	17.57
Alternate loading 1	17,161	.2872	-.003	11.16	17.73
Alternate loading 2	18,015	.2857	-.011	11.70	18.60

Loading	Moments of inertia, slug-ft^2				Mass parameters		
	I_p	I_X	I_Y	I_Z	$\dfrac{I_X - I_Y}{mb^2}$	$\dfrac{I_Y - I_Z}{mb^2}$	$\dfrac{I_Z - I_X}{mb^2}$
Basic loading	33	22,322	34,508	49,313	-92×10^{-4}	-112×10^{-4}	204×10^{-4}
Alternate loading 1	33	34,737	34,641	63,282	0	-212	212
Alternate loading 2	33	48,575	34,123	77,828	103	-310	207

CHART 1.- RIGHT SPIN AND RECOVERY CHARACTERISTICS OF MODEL FOR BASIC LOADING

[Recovery attempted by rapid full rudder reversal. Recovery attempted from, and steady-spin data presented for,
rudder full with spins. Model values converted to corresponding full-scale values.]

Flywheel not rotating

Flywheel rotating

(a)

(b)

67	2U
195	0.34
2, 2, 2½	

58	3D
208	0.32
½,	1½

56	5D
208	0.32
1, 1, 2	

62	0
208	0.40
1¾, 3, >4	

54	3D
211	0.39
2½, 3½, 4¾	

57	6D
208	0.41
2½,	3

Elevator full up (Stick back)

55	2D
195	0.39
2,	2¾

Ailerons full against (Stick left)

Ailerons full with (Stick right)

61	2D
186	0.47
∞	

Elevator full down (Stick forward)

64	3D
186	0.39
5, 5	

62	2D
186	0.48
∞	

[a]Moderately wandering spin.

[b]Whipping spin.

U   inner wing up
D   inner wing down

α (deg)	ϕ (deg)
V (fps)	Ω (rps)
Turns for recovery	

CHART 2.- LEFT SPIN AND RECOVERY CHARACTERISTICS OF MODEL FOR BASIC LOADING

[Recovery attempted by rapid full rudder reversal. Recovery attempted from, and steady-spin data presented for, rudder full with spins. Model values converted to corresponding full-scale values.]

Flywheel not rotating

Flywheel rotating

52	4U
224	0.30
1,	$1\frac{1}{2}$

53	6D
218	0.31
1,	$1\frac{1}{4}$

(a)

47	7D
Approx 227	
1,	$1\frac{1}{2}$

57	0
202	0.26
1,	$1\frac{1}{4}$

55	6D
202	0.26
1, 1,	$1\frac{1}{4}$

(a)

59	10D
221	0.27
$\frac{1}{2}$,	$\frac{3}{4}$, 1

Elevator full up (Stick back)

50	4D
221	0.38
$1\frac{1}{2}$,	$1\frac{3}{4}$

Ailerons full against (Stick right)

Ailerons full with (Stick left)

Elevator full down (Stick forward)

52	2D
211 192	0.38
2,	$2\frac{1}{2}$

Elevator full up (Stick back)

64	5D
189	0.32
$1\frac{1}{2}$, 2, 3	

Ailerons full against (Stick right)

Ailerons full with (Stick left)

Elevator full down (Stick forward)

66	4D
192	0.33
$1\frac{1}{2}$, 3, 4	

a Very wandering spin.

U inner wing up
D inner wing down

α (deg)	ϕ (deg)
V (fps)	Ω (rps)
Turns for recovery	

CHART 3.- RIGHT SPIN AND RECOVERY CHARACTERISTICS OF MODEL FOR ALTERNATE LOADING 1

[Recovery attempted by rapid full rudder reversal. Recovery attempted from, and steady-spin data presented for, rudder full with spins. Model values converted to corresponding full-scale values.]

Flywheel not rotating

Flywheel rotating

Two conditions

(a)

55	2U	72	3D
211	0.32	189	0.36
2, 3		1, 2, 3	

56	3D
208	0.32
3½,	4½

60	5D
208	0.32
2,	3, 3

58	0
208	0.40
3,	4, 10

61	2D
208	0.40
∞	

62	2D
208	0.43
∞	

Elevator full up (Stick back)

70	0
186	0.42
5½,	6½

Ailerons full against (Stick left)

69	2D
186	0.40
∞	

Ailerons full with (Stick right)

66	1D
186	0.52
8½,	9

Ailerons full against (Stick left)

64	1D
192	0.47
∞	

Ailerons full with (Stick right)

Elevator full down (Stick forward)

72	2D
176	0.44
7½,	9

67	0
186	0.41
∞	

68	0
186	0.50
>4,	8

63	2D
186	0.48
∞	

[a] Very wandering spin.

α (deg)	ϕ (deg)
V (fps)	Ω (rps)
Turns for recovery	

U   inner wing up
D   inner wing down

CHART 4.- LEFT SPIN AND RECOVERY CHARACTERISTICS OF MODEL FOR ALTERNATE LOADING 1

[Recovery attempted by rapid full rudder reversal. Recovery attempted from, and steady-spin data presented for, rudder full with spins. Model values converted to corresponding full-scale values.]

Flywheel not rotating

Flywheel rotating

(a)

55	1U
224	0.31
1, $1\frac{1}{4}$, $1\frac{1}{2}$	

56	2D
208	0.32
$1\frac{1}{2}$, 2	

61	1D
208	0.33
$1\frac{1}{2}$, 2	

Elevator full up (Stick back)

67	0
176	0.40
$3\frac{1}{2}$, 4	

← Ailerons full against (Stick right)

63	2D
192	0.39
$3\frac{1}{2}$, 4	

Ailerons full with (Stick left) →

Elevator full down (Stick forward)

69	1D
176	0.41
$4\frac{1}{2}$, 5	

62	1D
186	0.40
4, 5	

(b)

72	2D
186	0.32
2, $2\frac{1}{4}$	

59	4D
208	0.27
2, 2, $2\frac{1}{4}$	

57	5D
208	0.27
1, $1\frac{1}{4}$	

Elevator full up (Stick back)

74	3D
182	0.35
4, 5	

← Ailerons full against (Stick right)

67	2D
182	0.35
4, $4\frac{1}{2}$	

Ailerons full with (Stick left) →

Elevator full down (Stick forward)

74	2D
182	0.38
8, 9	

68	3D
186	0.35
5, 9	

[a]Slightly wandering spin.
[b]Wandering and whipping spin.

U   inner wing up
D   inner wing down

α (deg)	φ (deg)
V (fps)	Ω (rps)
Turns for recovery	

CHART 5.- RIGHT SPIN AND RECOVERY CHARACTERISTICS OF MODEL FOR ALTERNATE LOADING 2

[Recovery attempted by rapid full rudder reversal. Recovery attempted from, and steady-spin data presented for, rudder full with spins. Model values converted to corresponding full-scale values.]
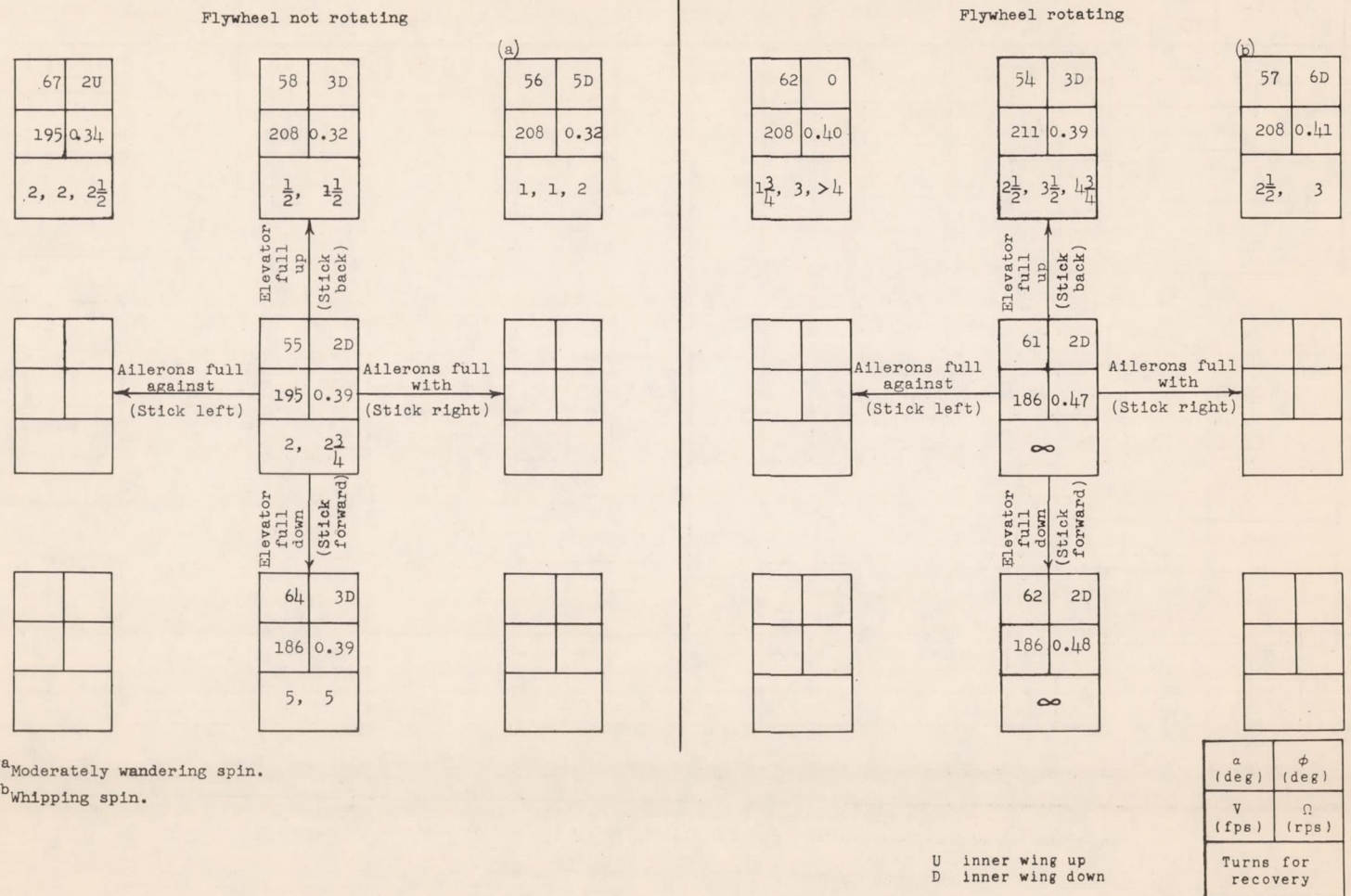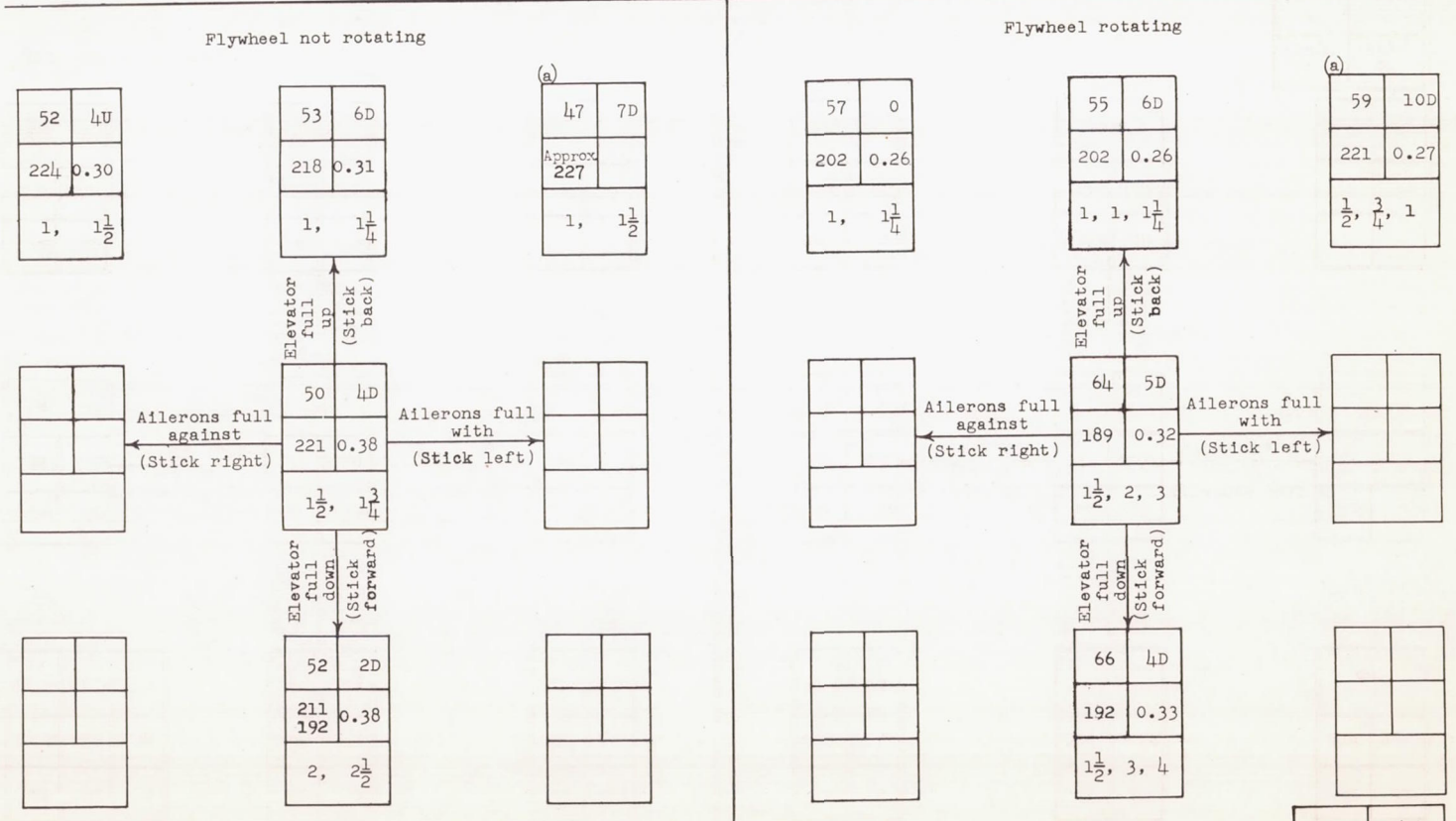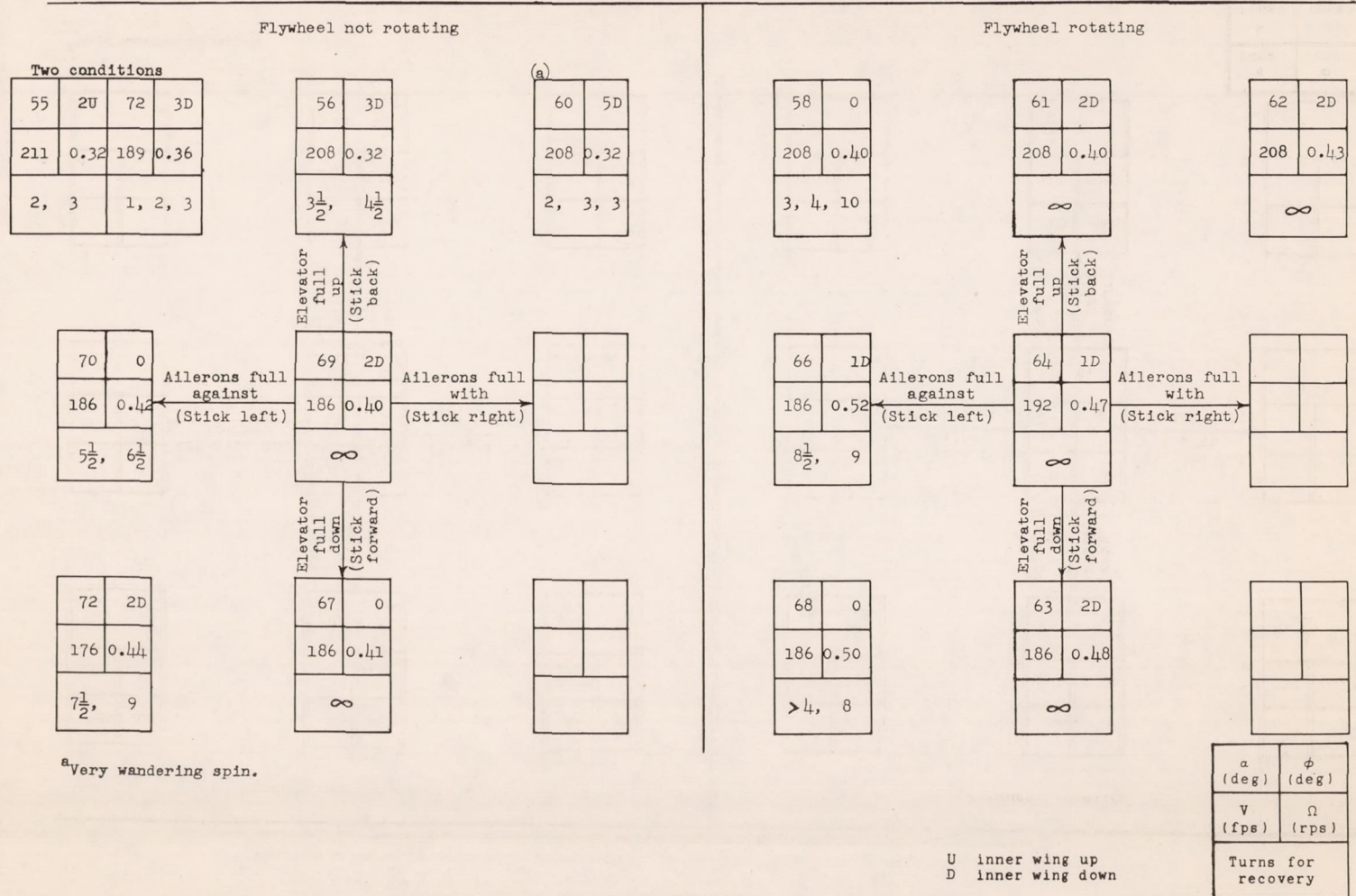
Flywheel not rotating

65	1D
202	0.41
$3\frac{1}{2}$, $3\frac{3}{4}$	

49	2D
218	0.34
∞	

51	2D
218	0.34
>8	

Elevator full up (Stick back)

64	0
182	0.44
$4\frac{1}{2}$, 5	

Ailerons full against (Stick left)

62	1D
186	0.43
∞	

Ailerons full with (Stick right)

61	2D
192	0.42
∞	

Elevator full down (Stick forward)

62	1U
189	0.45
$5\frac{1}{2}$, $6\frac{1}{4}$	

61	2D
189	0.43
>9	

55	1D
192	0.42
>9	

Flywheel rotating

41	1U
234	0.38
$1\frac{3}{4}$, $2\frac{1}{2}$	

48	1D
208	0.41
∞	

51	3D
218	0.41
∞	

Elevator full up (Stick back)

55	2U
198	0.47
$5\frac{1}{4}$, $6\frac{1}{4}$	

Ailerons full against (Stick left)

56	1U
189	0.49
∞	

Ailerons full with (Stick right)

55	2D
179	0.49
∞	

Elevator full down (Stick forward)

57	0
192	0.48
$5\frac{1}{2}$, $11\frac{1}{2}$	

56	1D
189	0.50
∞	

54	1D
192	0.48
∞	

U inner wing up
D inner wing down

a (deg)	ϕ (deg)
V (fps)	Ω (rps)
Turns for recovery	

CHART 6.- LEFT SPIN AND RECOVERY CHARACTERISTICS OF MODEL FOR ALTERNATE LOADING 2

[Recovery attempted by rapid full rudder reversal. Recovery attempted from, and steady-spin data presented for, rudder full with spins. Model values converted to corresponding full-scale values.]
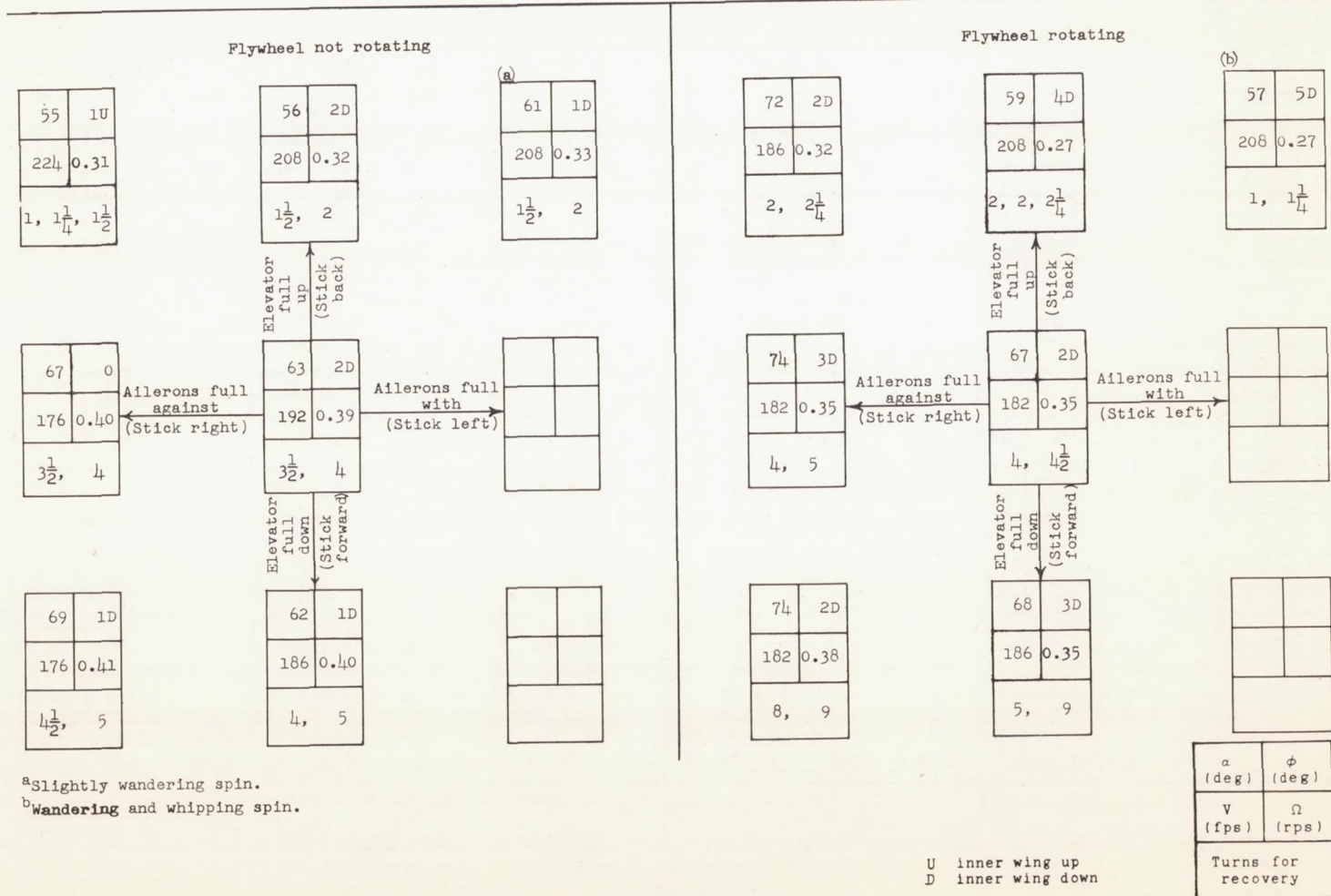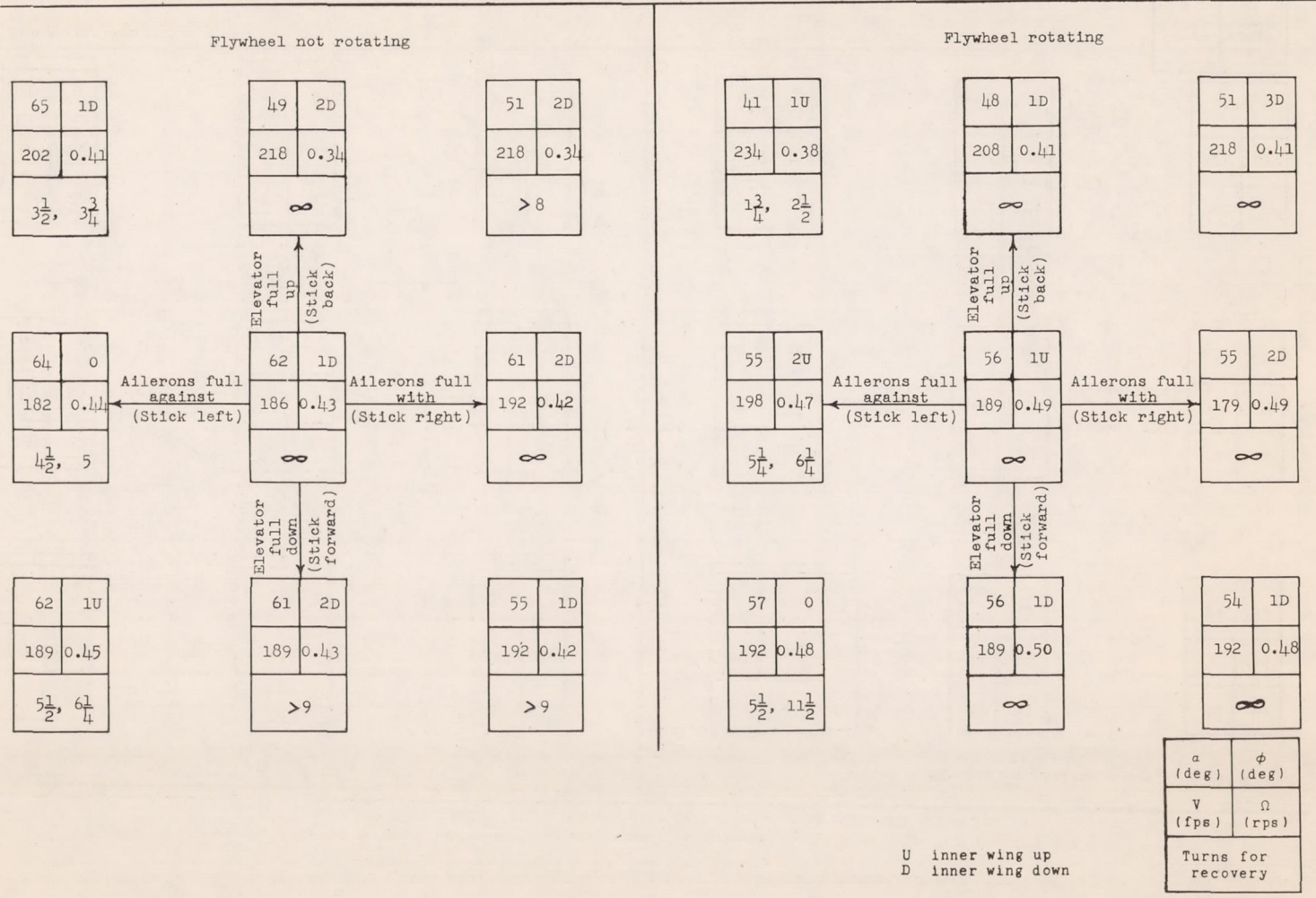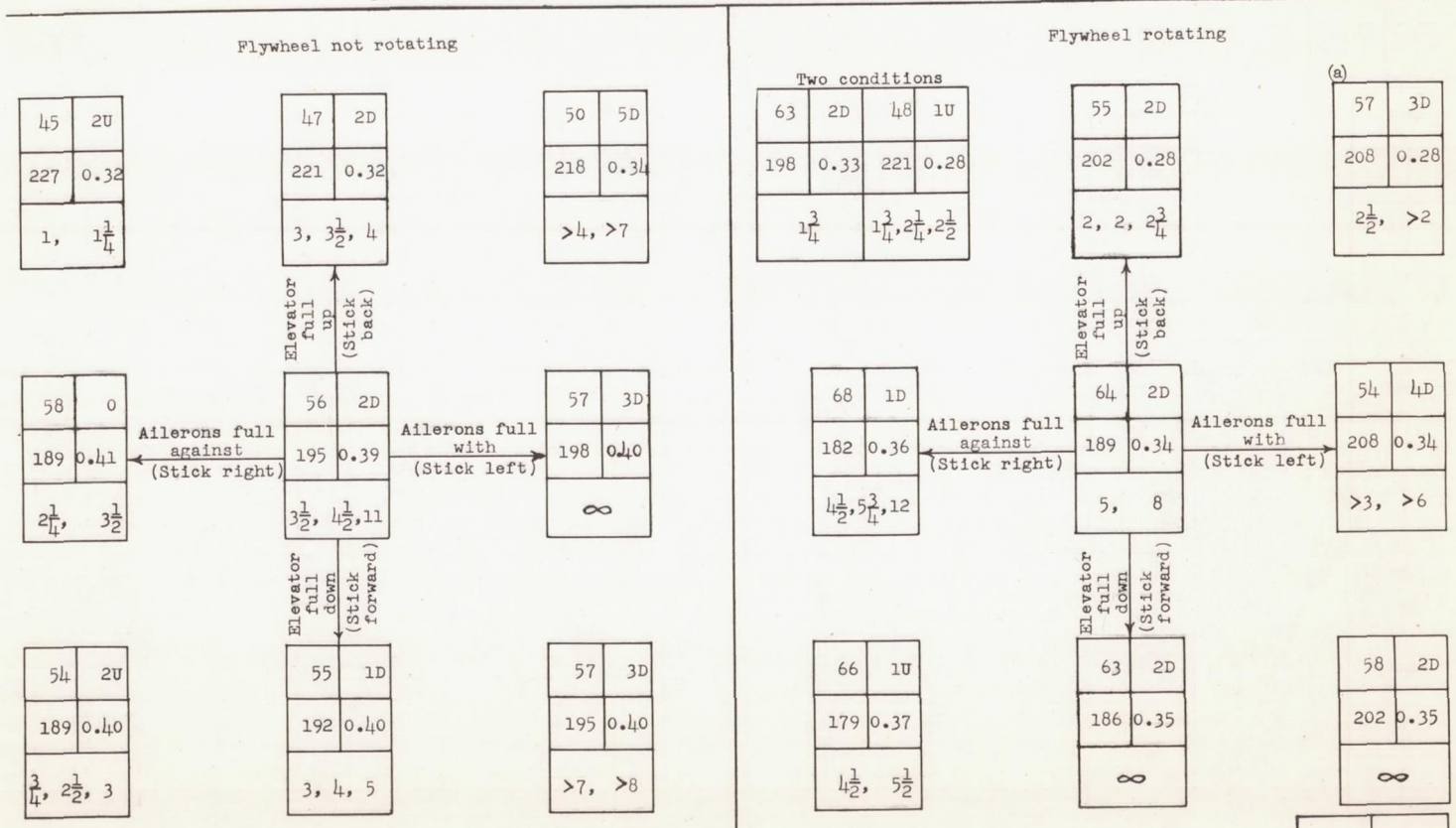
Flywheel not rotating

45	2U
227	0.32
1,	$1\frac{1}{4}$

47	2D
221	0.32
3,	$3\frac{1}{2}$, 4

50	5D
218	0.34
>4, >7	

Elevator full up (Stick back)

58	0
189	0.41
$2\frac{1}{4}$,	$3\frac{1}{2}$

←— Ailerons full against (Stick right)

56	2D
195	0.39
$3\frac{1}{2}$, $4\frac{1}{2}$, 11	

Ailerons full with (Stick left) —→

57	3D
198	0.40
∞	

Elevator full down (Stick forward)

54	2U
189	0.40
$\frac{3}{4}$, $2\frac{1}{2}$, 3	

55	1D
192	0.40
3, 4, 5	

57	3D
195	0.40
>7, >8	

ᵃMorderately wandering spin.

Flywheel rotating

Two conditions

63	2D	48	1U
198	0.33	221	0.28
$1\frac{3}{4}$		$1\frac{3}{4}$, $2\frac{1}{4}$, $2\frac{1}{2}$	

55	2D
202	0.28
2, 2, $2\frac{3}{4}$	

(a)

57	3D
208	0.28
$2\frac{1}{2}$, >2	

Elevator full up (Stick back)

68	1D
182	0.36
$4\frac{1}{2}$, $5\frac{3}{4}$, 12	

←— Ailerons full against (Stick right)

64	2D
189	0.34
5, 8	

Ailerons full with (Stick left) —→

54	4D
208	0.34
>3, >6	

Elevator full down (Stick forward)

66	1U
179	0.37
$4\frac{1}{2}$, $5\frac{1}{2}$	

63	2D
186	0.35
∞	

58	2D
202	0.35
∞	

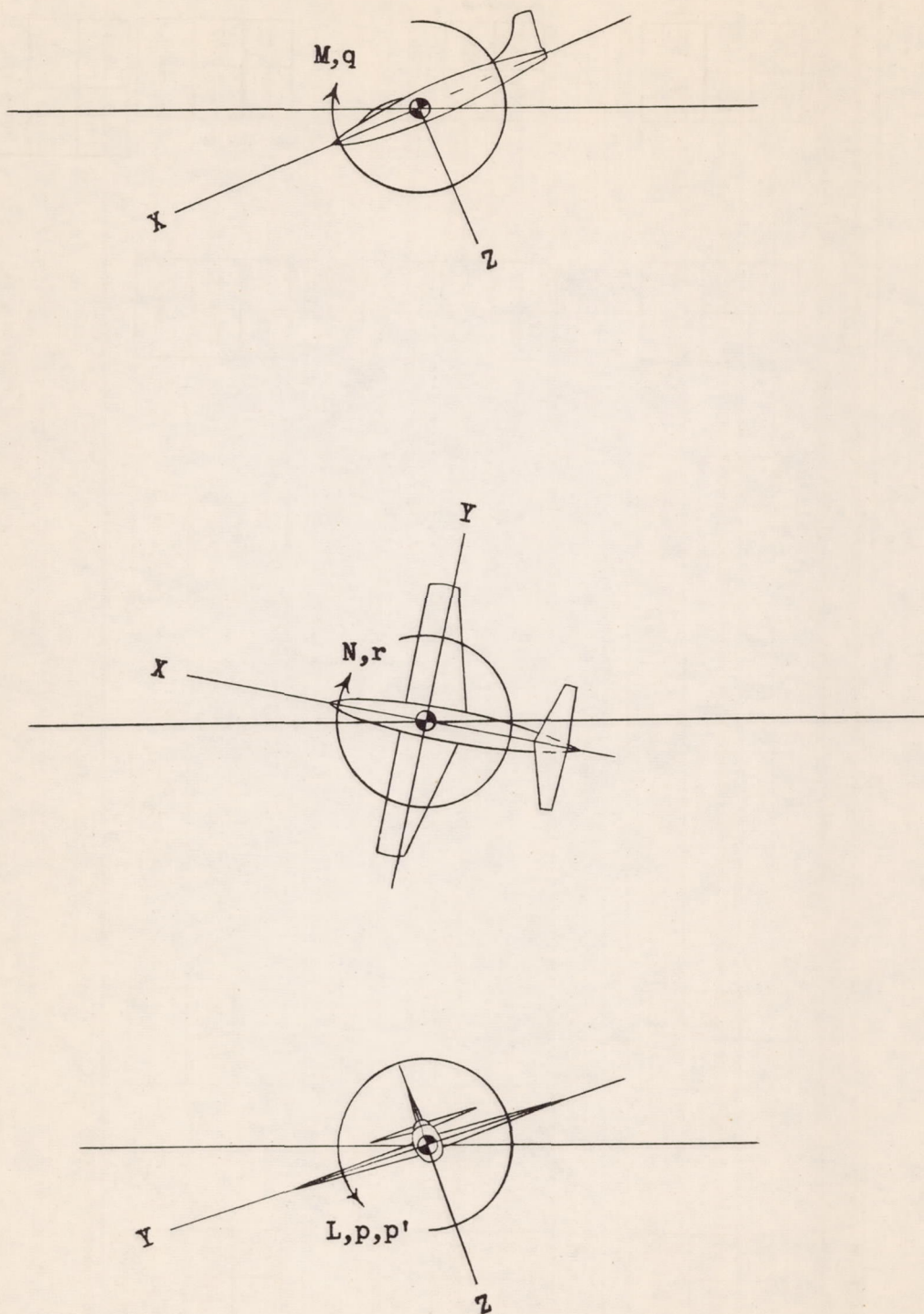| α (deg)	ϕ (deg)
V (fps)	Ω (rps)
Turns for recovery	

U inner wing up
D inner wing down

Figure 1.- Sketch showing positive directions of moments and angular
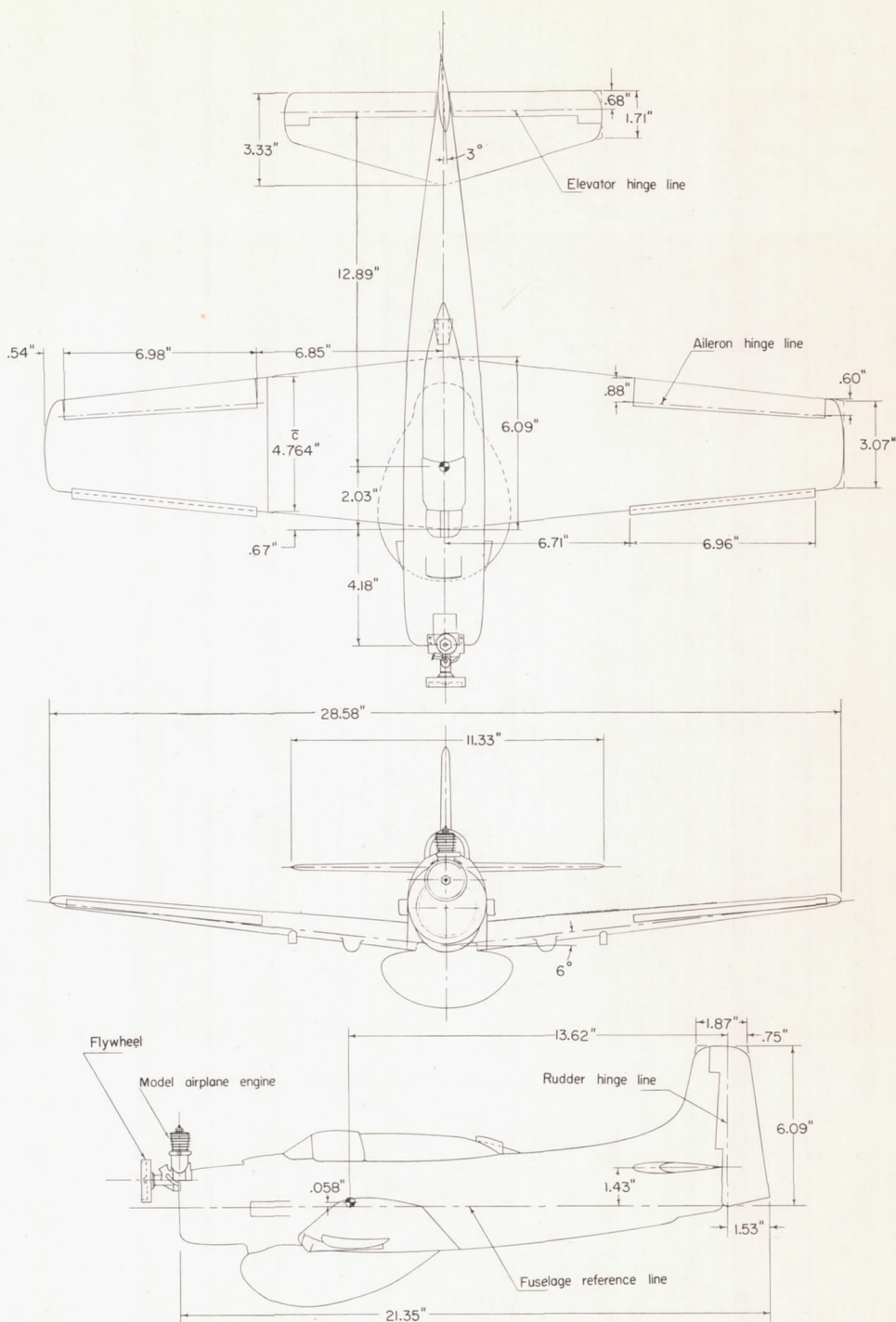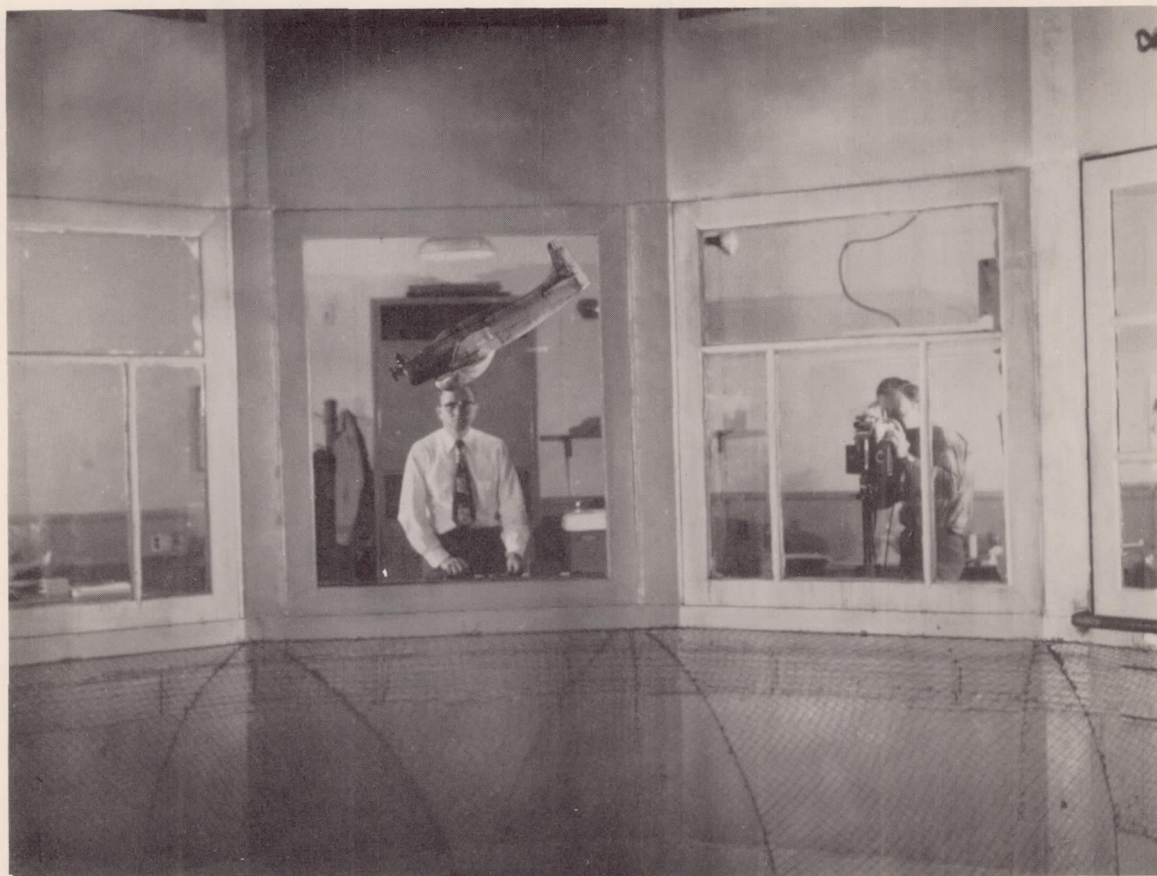velocities about body system of axes.

Figure 2.- Three-view drawing of a 1/21-scale model of a military attack
   airplane used for gyroscopic-moment tests in Langley 20-foot free-
   spinning tunnel. Dimensions are model values. Center-of-gravity
   position shown is for alternate loading 2.

L-82629

Figure 3.- Photograph of model spinning in Langley 20-foot free-spinning tunnel.

NACA - Langley Field, Va.